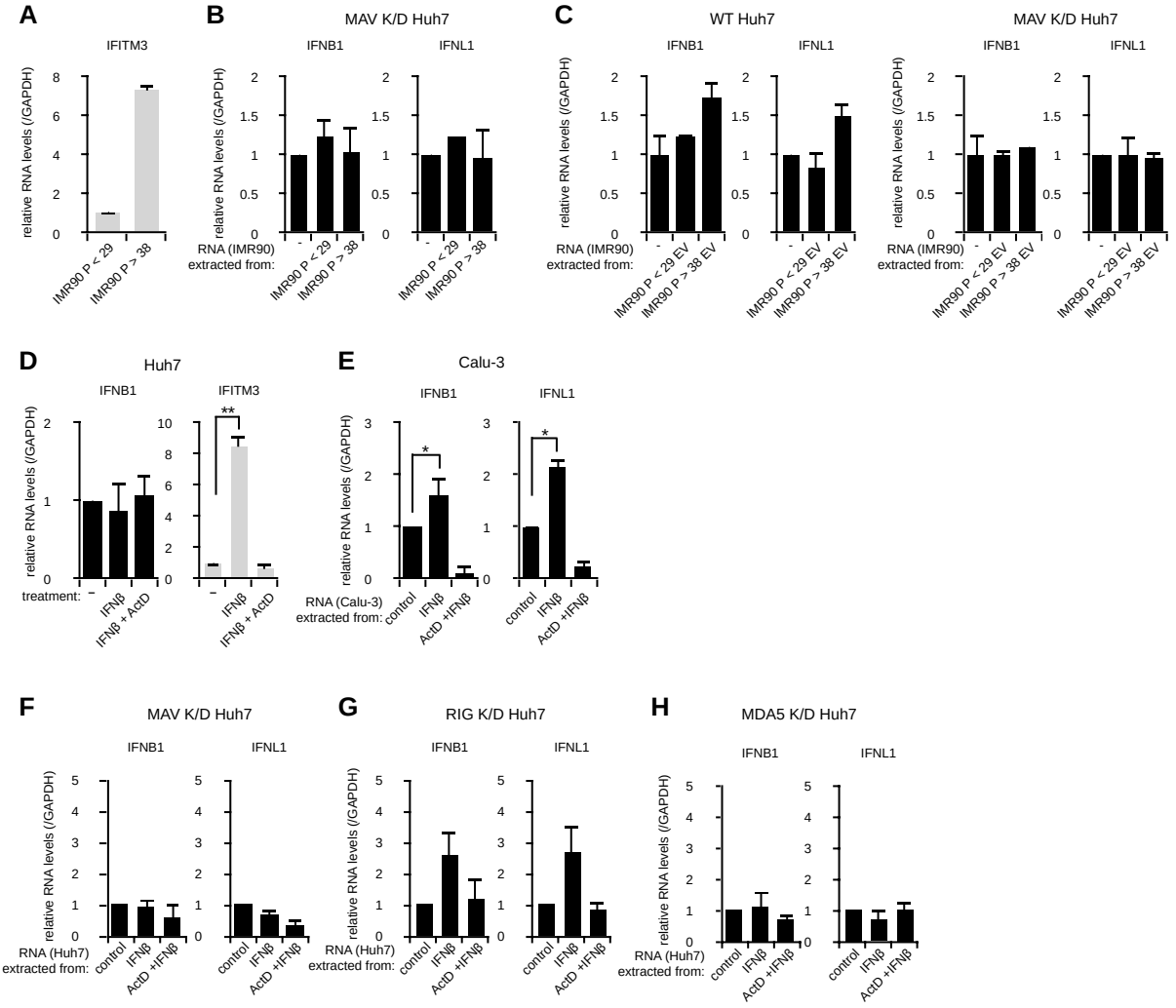


**Figure S1. RNA transcripts from senescent cells and IFN-induced RNA transcripts induce type I IFN through MDA5.**

(**A**) Expression levels of IFITM3 mRNA were examined in IMR90 fibroblasts (P<29 or P>38). **(B)** mRNA abundance of IFNB1 and IFNL1 was monitored in MAVS K/D Huh7 cells (n=2) which were transfected with RNA extracts from IMR90 fibroblasts (P<29 or P>38). **(C)** mRNA abundance of IFNB1 and IFNL1 was monitored in WT or MAVS K/D Huh7 cells (n=2) which were transfected with EV RNA from IMR90 CCM (P<29 or P>38). CCM: cell conditional medium. EV: exosomal vehicle. (**D**) Expression levels of IFNB1 and IFITM3 mRNA in untreated, IFNβ-treated, and IFNβ/ActD-treated Huh7 cells (n = 4) were examined 24 hrs post-treatments. (**E**) Quantification of IFNB1 or IFNL1 mRNA by qRT-PCR in Calu-3 cells (n = 3) which were transfected with RNA extracts from IFNβ-treated, IFNβ/ActD-treated, or untreated Calu-3 cells. (**F**)(**G**)(**H**) Total RNA was extracted from IFNβ-treated, IFNβ/ActD-treated, or untreated WT Huh7 cells. These RNA extracts were transfected into MAVS K/D **(F)**, RIG-I K/D **(G)** and MDA5 K/D Huh7 cells **(H)** respectively. IFNB1 and IFNL1 mRNA expression levels in transfected MAVS K/D (n = 4), RIG-I K/D (n = 4) and MDA5 K/D (n = 3) Huh7 cells were monitored by qRT-PCR. Data are mean + SEM. Statistical analysis was performed using Mann-Whitney U test or student t-test.

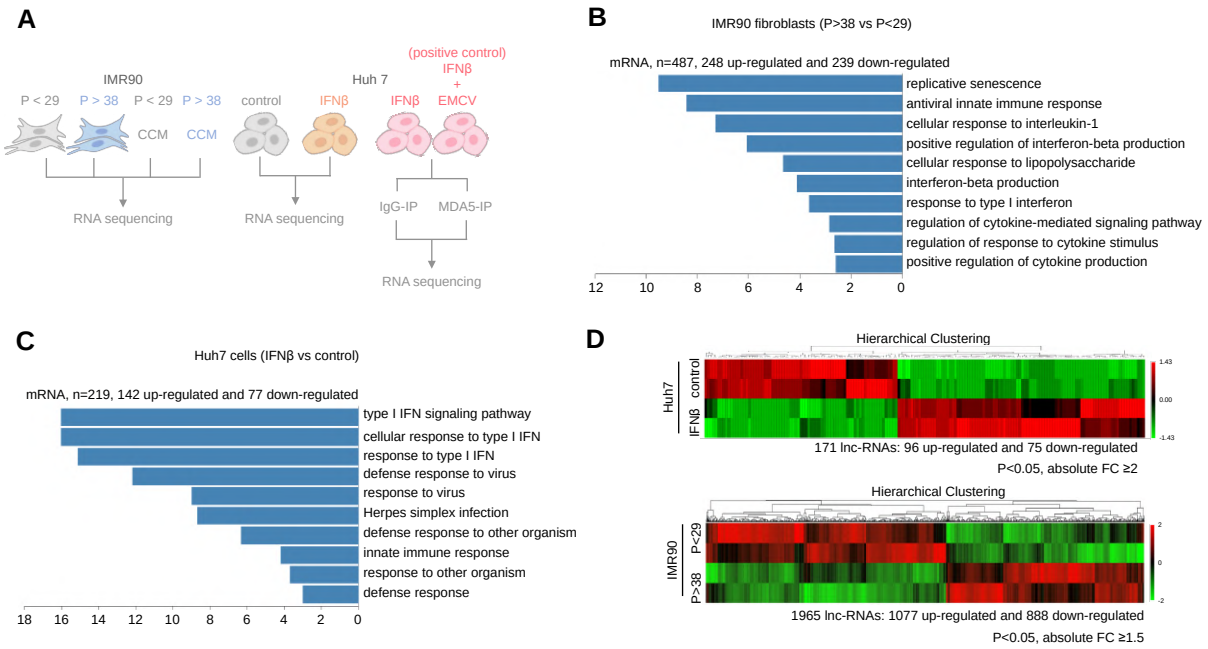


E

| | Input (IFNβ vs Mock) | | IP (IFNβ anti-MDA5 vs IFNβ IgG) | |
|---|---|---|---|---|
| Column ID | p-value | Fold-Change | p-value | Fold-Change |
| lnc-CCDC122-2:1 | 0.003 | 5.166 | 0.014 | 5.486 |
| lnc-TMEM14A-1:7 | 0.032 | 42.569 | 0.025 | 1.82E+07 |
| lnc-TMEM14A-1:3 | 0.032 | 42.568 | 0.025 | 1.82E+07 |
| lnc-FBXW4-1:2 | 0.065 | 2.041 | 0.012 | 47.864 |
| CATIP-AS2:2 | 0.081 | 8.691 | 0.038 | 11.984 |

F

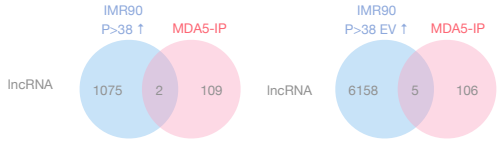


G

| | IMR90 (P > 38 vs P < 29) | | IP (IFNβ anti-MDA5 vs IFNβ IgG) | |
|---|---|---|---|---|
| Column ID | p-value | Fold-Change | p-value | Fold-Change |
| lnc-PIGC-4:1 | 0.027 | 1.565 | 0.007 | 8.540 |
| lnc-CCDC122-2:1 | 0.023 | 1.814 | 0.014 | 5.486 |

| | IMR90 EV (P > 38 vs P < 29) | | IP (IFNβ anti-MDA5 vs IFNβ IgG) | |
|---|---|---|---|---|
| Column ID | p-value | Fold-Change | p-value | Fold-Change |
| lnc-MTERF1-8:1 | 0.016 | 1.946 | 0.015 | 3.690 |
| TIPARP-AS1:2 | 0.003 | 2.082 | 0.008 | 2.34E+05 |
| CATIP-AS2:2 | 0.025 | 1.845 | 0.038 | 11.984 |
| lnc-GPS1-2:1 | 0.001 | 2.012 | 0.025 | 4.34E+10 |
| lnc-HFM1-4:8 | 0.007 | 1.621 | 0.035 | 4.32E+04 |

H

| Sequence Name | RNA size | ORF size | Ficket Score | Hexamer Score | Coding Probability | Coding Label | Alu-element |
|---|---|---|---|---|---|---|---|
| lnc-CCDC122-2:1 | 704 | 375 | 0.8375 | -0.0488545 | 0.1447441 | no | None |
| CATIP-AS2:2 | 1183 | 354 | 0.6442 | 0.0137708 | 0.09740278 | no | None |

**Figure S2. MDA5-bound lncRNAs are identified via MDA5-RNA IP RNA-sequencing.**

(**A**) Illustration of experimental design for RNA-sequencing. RNA-sequencing analyzed the mRNA and lncRNA abundance in IMR90 fibroblasts (P<29 or P>38) (n=2), IMR90 CCM (P<29 or P>38) (n=2), Huh7 cells (control or IFNβ treatment) (n=2) and antibody-immunoprecipitants (anti-IgG or anti-MDA5 RNA-IP) (n=3). EMCV viral RNA served as positive control of anti-MDA5 RNA-IP (n=3). **(B)** Ontology analysis of IMR90 fibroblasts (P>38 vs P<29) from RNA-sequencing. (**C**) Ontology analysis of Huh7 cells (IFNβ vs control) from RNA-sequencing. **(D)** Hierarchical clustering analysis of lncRNAs (absolute fold-changes > 2-fold, $p < 0.05$) in total RNA from control and IFNβ treated Huh7 cells or lncRNAs (absolute fold-changes > 1.5-fold, $p < 0.05$) in total RNA from P>38 and P<29 IMR90 fibroblasts. (**E**) lncRNA candidates were selected based on the intersection of two criteria: (1) their expression was induced by IFNβ, and (2) interaction with MDA5 was detected. Candidates showing non-specific interactions in IgG controls were excluded. **(F)** Venn

diagrams showed two lncRNA candidates were increased in IMR90 fibroblasts P<38 (left circle) and interacted with MDA5 in Huh7 cells (right circle). lncRNA candidates were listed below. **(G)** Venn diagrams showed lncRNA candidates were increased in IMR90 fibroblasts P<38 EV (left circle) and interacted with MDA5 in Huh7 cells (right circle). lncRNA candidates were listed below. EV: exosomal vehicle. Data are mean + SEM. Statistical analysis was performed using Mann-Whitney U test or student t-test. **(H)** Coding probability off lnc-CCDC122-2:1 and CATIP-AS2:2 was predicted by Coding Potential Assessment Tool (CPAT). The coding probability is calculated according to the open reading frame size, open reading frame coverage, Fickett TESTCODE statistic and hexamer usage bias[1].

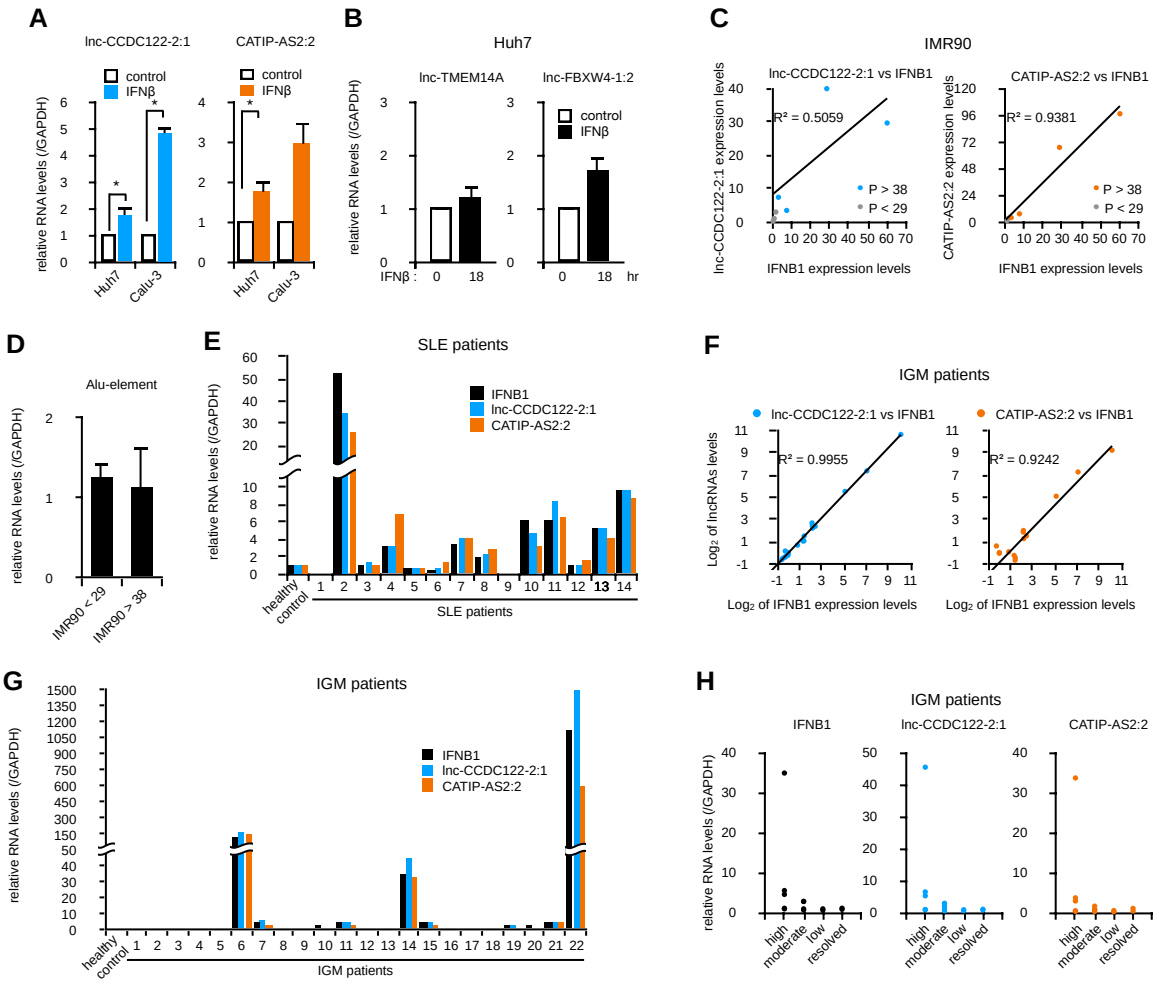


**Figure S3. High expressions of Lnc-CCDC122-2:1 and CATIP-AS2:2 in autoimmune diseases.**

**(A)** RNA expression levels of lnc-CCDC122-2:1 and CATIP-AS2:2 were quantified by qRT-PCR in Huh7 cells (n = 4) or Calu-3 cells (n = 4) treated with IFNβ for 18 hours. (**B**) RNA expressions levels of lnc-TMEM14A (n = 4) and lnc-FBXW4-1:2 (n = 3) selected from (supfig. 2E) were quantified by qRT-PCR in Huh7 cells with or without IFNβ treatment. (**C**) Correlations between lncCCDC122-2:1 or CATIP-AS2:2 RNA and IFNB1 mRNA in P>38 or P<29 IMR90 fibroblasts illustrated the scatter plot. R square showed the correlation between target RNA and IFNB1. P: passage numbers. **(D)** Abundance of Alu-element containing RNA was detected by qPCR in IMR90 fibroblasts (P<29 or P>38). **(E)** RNA was extracted from PBMC of systemic lupus erythematosus (SLE) and healthy donors. IFNB1 mRNA, lncCCDC122-2:1 RNA, and CATIP-AS2:2 RNA abundance was detected by qRT-PCR. **(F)** Scatter plot showed the correlation between IFNB1 mRNA levels and lncCCDC122-2:1 RNA or CATIP-AS2:2 RNA levels. **(G)** RNA was extracted from idiopathic granulomatous mastitis (IGM) patients and healthy donors. IFNB1 mRNA, lncCCDC122-2:1 RNA, and CATIP-AS2:2 RNA abundance was detected by qRT-PCR. **(H)** IGM patients from (**E**) excluded samples with positive bacteria isolation were classified into four different disease severity. IFNB1 mRNA, lnc-CCDC122-2:1, and CATIP-AS2:2 were detected by qRT-PCR in PBMC from these classiied IGM patients (n = 1). Data are mean + SEM. Statistical analysis was performed using Mann-Whitney U test or student t-test.

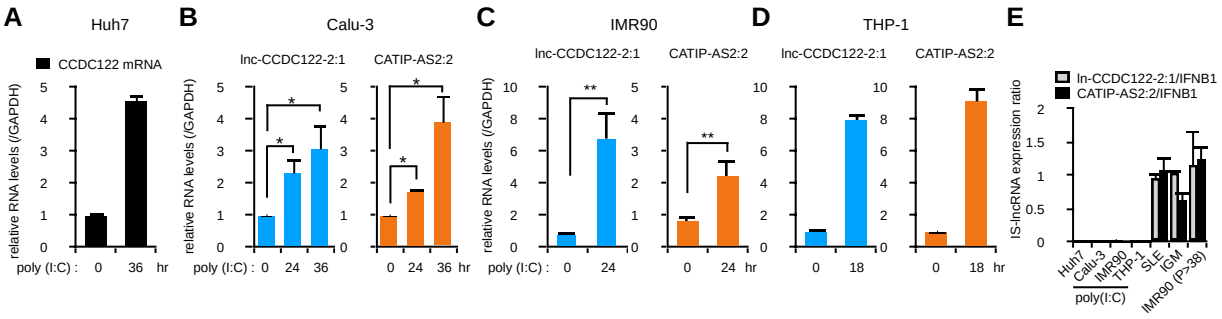


**Figure S4. High molecular-weight synthetic dsRNA, poly (I:C), transiently induces lnc-CCDC122-2:1 and CATIP-AS2:2.**

**(A)** Quantification of CCDC122 mRNA amounts by qRT-PCR in Huh7 cells treated with HMW poly (I:C). **(B)(C)(D)** Quantification of RNA expression levels of lnc-CCDC122-2:1 and CATIP-AS2:2 by qRT-PCR in Calu-3 cells (n = 3) (B), IMR90 fibroblasts (n = 7) (D) or THP-1 cells (C), treated with HMW poly (I:C) for 24 hours (C), 18 hours (D), or at indicated time points (B). (**E**) RNA ratio of lncCCDC122-2:1/IFNB1 or CATIP-AS2:2/IFNB1 were calculated in Huh7 cells, Calu-3 cells and P<29 IMR90 fibroblasts with poly (I:C) treatment. The ratios were also calculated in PMBC from SLE and IGM, and in P>38 IMR90 fibroblasts. P: passage numbers. Data are mean + SEM. Statistical analysis was performed using Mann-Whitney U test or student t-test.

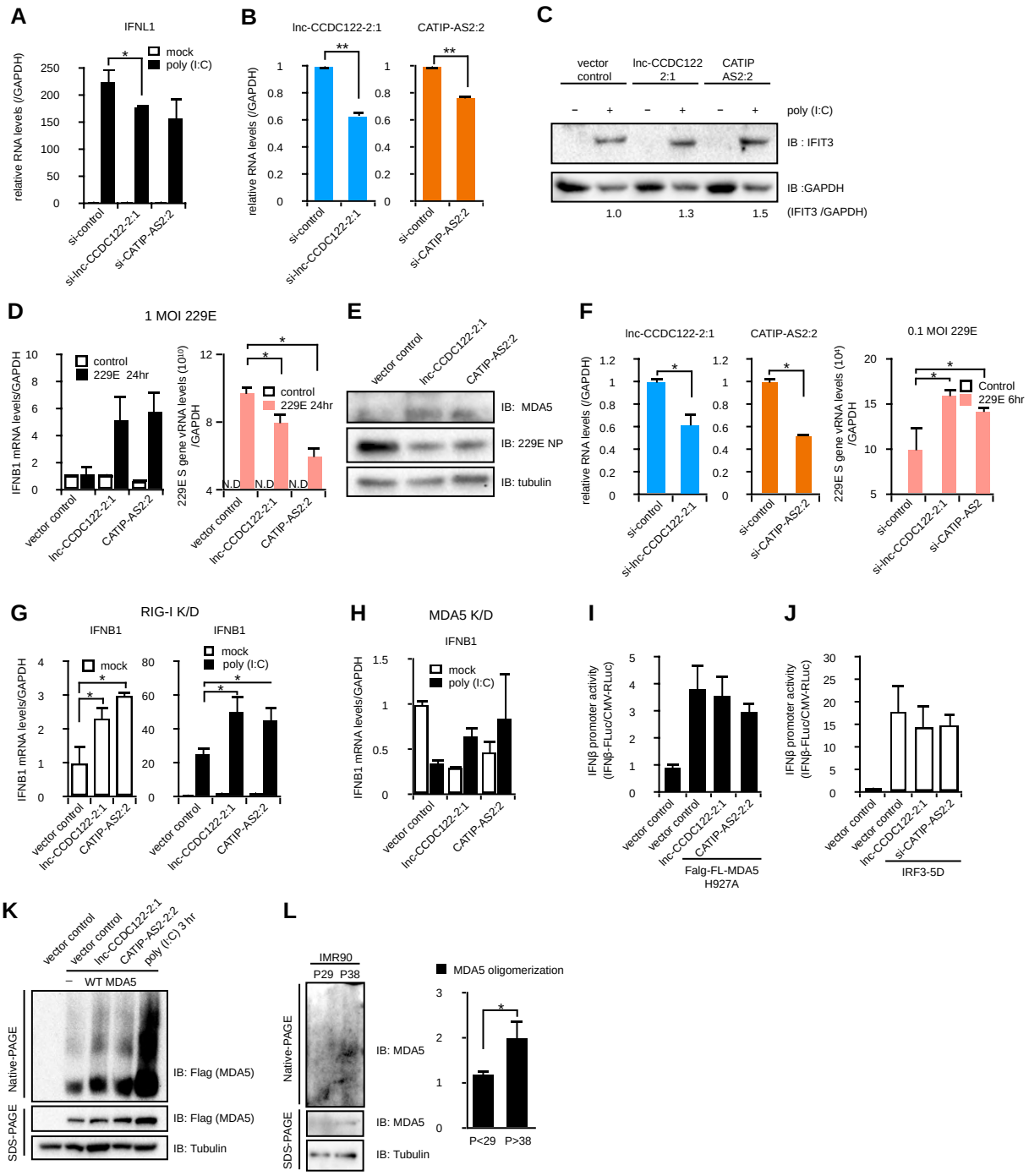


**Figure S5. Lnc-CCDC122-2:1 and/or CATIP-A2:2 primes MDA5 aggregation to induce type I IFN and inhibit viral replication.**

(**A**) Quantification of lnc-CCDC122-2:1 and CATIP-AS2:2 by qRT-PCR showing siRNA knockdown efficiency in Huh7 cells transfected with si-lncCCDC122-2:1, or CATIP-AS2:2 siRNA for 60 hours (n = 3). (**B**) Abundance of IFNL1 mRNA transcripts were detected by qRT-PCR in Huh7 cells transfected with si-control, si-lncCCDC122-2:1, or CATIP-AS2:2 siRNA for 24 hours then followed by poly (I:C) stimulation for 36 hours. (**C**) Abundance of IFIT3 proteins was measured by immunoblotting in vector control-, lncCCDC122-2:1, or CATIP-AS2:2-transfected Huh7 cells (n = 4) co-stimulated with HMW poly (I:C) transfection for 36 hours. (**D**) IFNB1 mRNA, 229E viral RNA of S gene were monitored by qRT-PCR in vector control, lnc-CCDC122-2:1, or CATIP-AS2:2 ectopically expressed Huh7 cells infected with 229E of 1 MOI (n = 3) for 24 hours. (**E**) MDA5 protein and 229E nucleoprotein (NP) levels were detected by immunoblotting in vector control, lnc-CCDC122-2:1, or CATIP-AS2:2 ectopically expressed Huh7 cells (n =

3) infected with 229E 0.1 MOI for 24 hours. (**F**) 229E S gene viral RNA was detected by qRT-PCR in WT Huh7 cells transfected with specific siRNA (si-control, si-lncCCDC122-2:1, or si-CATIP-AS2:2) for 48 hours followed by 0.1 MOI 229E infection for 6 hours. (**G**)(**H**) Quantification of IFNB1 mRNA by qRT-PCR in empty vector-, lncCCDC122-2:1-, or CATIP-AS2:2-transfected RIG-I K/D (D) (n = 3) or MDA5-K/D (E) (n = 3) Huh7 cells with or without poly HMW (I:C) transfection for 36 hours. (**I**) IFNβ promoter activity in Huh7 cells co-transfected with empty vector, lnc-CCDC122-2:1, or CATIP-AS2:2 with the same amount of Flag-FL-MDA5 H927A mutant (n = 3). (**J**) IFNβ promoter activity in Huh7 cells co-transfected with empty vector, lnc-CCDC122-2:1, or CATIP-AS2:2 plus a constant amount of IRF3-5D mutant (n = 2). (**K**) MDA5-oligomerization was determined by native-PAGE in Huh7 cells co-transfected with empty vector, lnc-CCDC122-2:1, or CATIP-AS2:2 plus a constant amount of Flag-FL-MDA5. HMW poly (I:C) treatment for 3 hours in Flag-MDA5 expressing cells served as a positive control of MDA5-oligomerization. (**L**) MDA5-oligomerization of P > 37 or P < 29 IMR90 fibroblasts were monitored by native-PAGE, and quantification data were averaged from 3 independent experiments. Data are mean + SEM. Statistical analysis was performed using Mann-Whitney U test or student t-test.

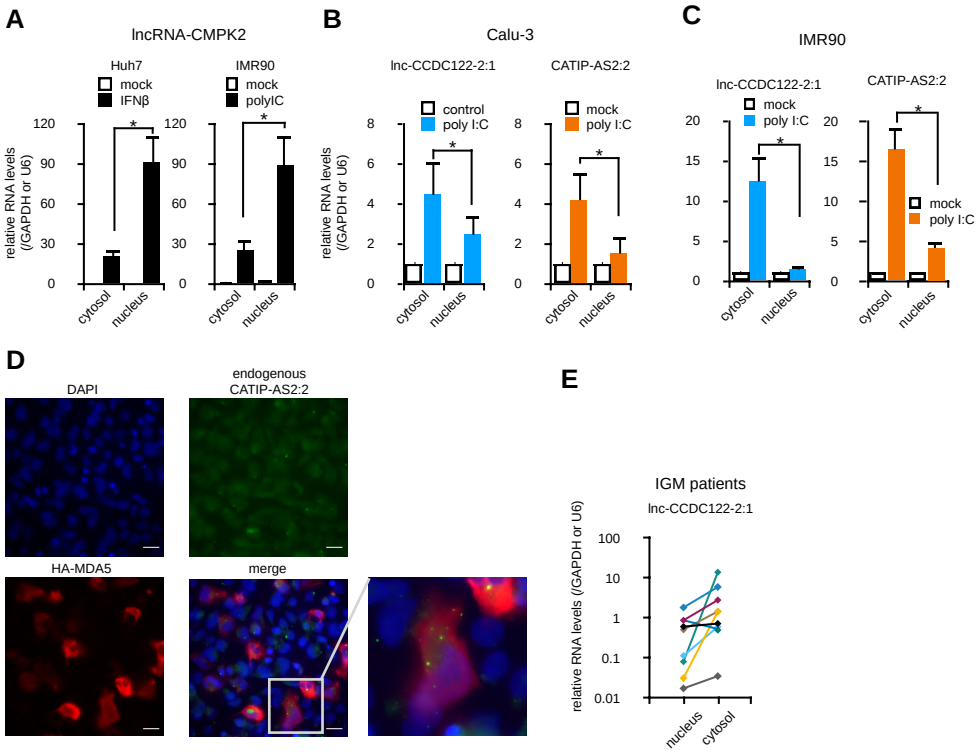


**Figure S6. Cytosolic distribution of lnc-CCDC122-2:1 and CATIP-AS2:2 are conserved across different human cell-lines and autoimmune diseases.**

**(A)** RNA abundance of lncCMPK2, a nuclear IFN-stimulated lncRNA, was detected by qRT-PCR as a control (n = 3). **(B)(C)** RNA amounts of lnc-CCDC122-2:1 and CATIP-AS2:2 were detected in cytosolic or nuclear fractions in calu-3 cells (B) (n = 4) and in IMR90 fibroblasts (C) (n = 3) transfected with or without poly(I:C) for 36 hours. (**D**) Huh7 cells were transfected with HA-MDA5. FISH images of CATIP-AS2:2 (green) and HA-MDA5 (red) in Huh7 cells treated with HMW poly (I:C) for 36 hours were detected by RNAscope and anti-HA-antibody. Nuclei were counterstained with DAPI (blue). Scale bars: 20 μm; original magnification, X60. OE: overexpression. (**E**) Lnc-CCDC122-2:1 RNA amount was detected in nuclear and cytosolic fractions in IGM patients and healthy donors. Cytosolic RNA or nuclear RNA abundance were normalized to cytosolic GAPDH mRNA or nuclear U6 RNA. All RNA in different fractions was compared to the RNA from the corresponding fractions in healthy donors. Data are mean + SEM. Statistical analysis was performed using Mann-Whitney U test or student t-test

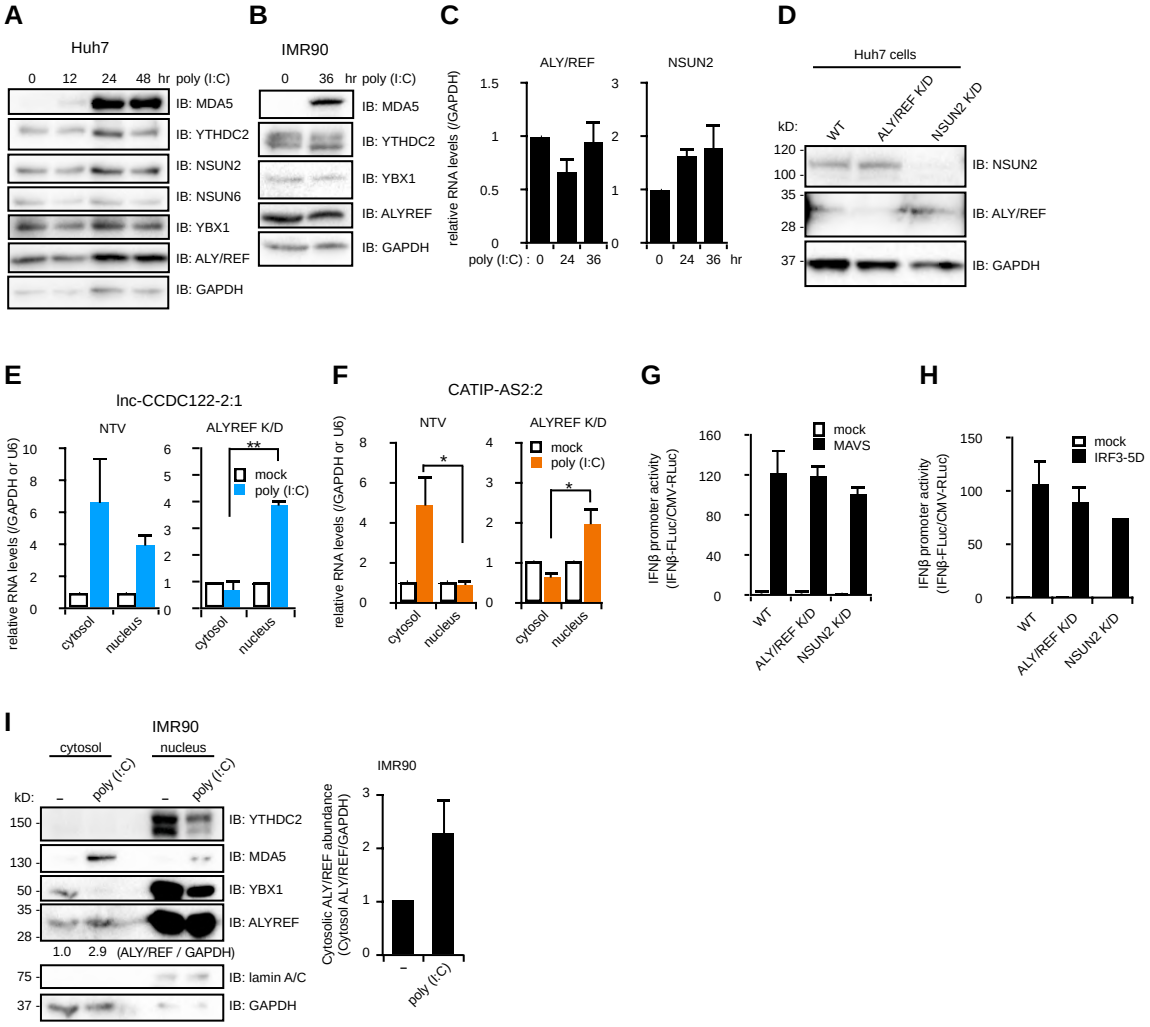


**Figure S7. ALY/REF promotes the kinetics of type I IFN induction by controlling nuclear exports of MDA5-bound lncRNAs**

(**A**) Abundance of MDA5, YTHDC2, NSUN2, NSUN6, YBX1, ALY/REF, and GAPDH were monitored by immunoblotting in Huh7 cells with poly (I:C) transfection at indicated time points. (**B**) Abundance of MDA5, YTHDC2, YBX1, ALY/REF, and GAPDH were monitored by immunoblotting in IMR90 fibroblasts with poly (I:C) transfection for 36 hours. (**C**) RNA amounts of NSUN2 (n = 4) and ALY/REF (n = 3) in Huh7 cells were monitored by qRT-PCR after poly (I:C) transfection at indicated time points. (**D**) Protein abundance of NSUN2, ALY/REF, and GAPDH were detected by immunoblotting in WT, NSUN2 K/D and ALY/REF K/D cells. (**E**)(**F**) RNA abundance of lnc-CCDC122-2:1 (E) or CATIP-AS2:2 (F) was detected by qRT-PCR in cytosolic and nuclear fractions from NTV (non-targeting vector) (n = 3) or ALY/REF K/D (n = 3) Huh7 cells transfected with or without poly(I:C) for 36 hours. (**G**)(**H**) IFNβ promoter activity induced by MAVS (G) (n = 3) or IRF3-5D (H) (n = 2) was measured in WT, NSUN2 K/D, and ALY/REF K/D Huh7 cells. (**I**) Protein level of cytosolic ALY/REF was quantified by normalization to cytosolic GAPDH in IMR90 fibroblasts (n = 2) transfected with or without poly (I:C).

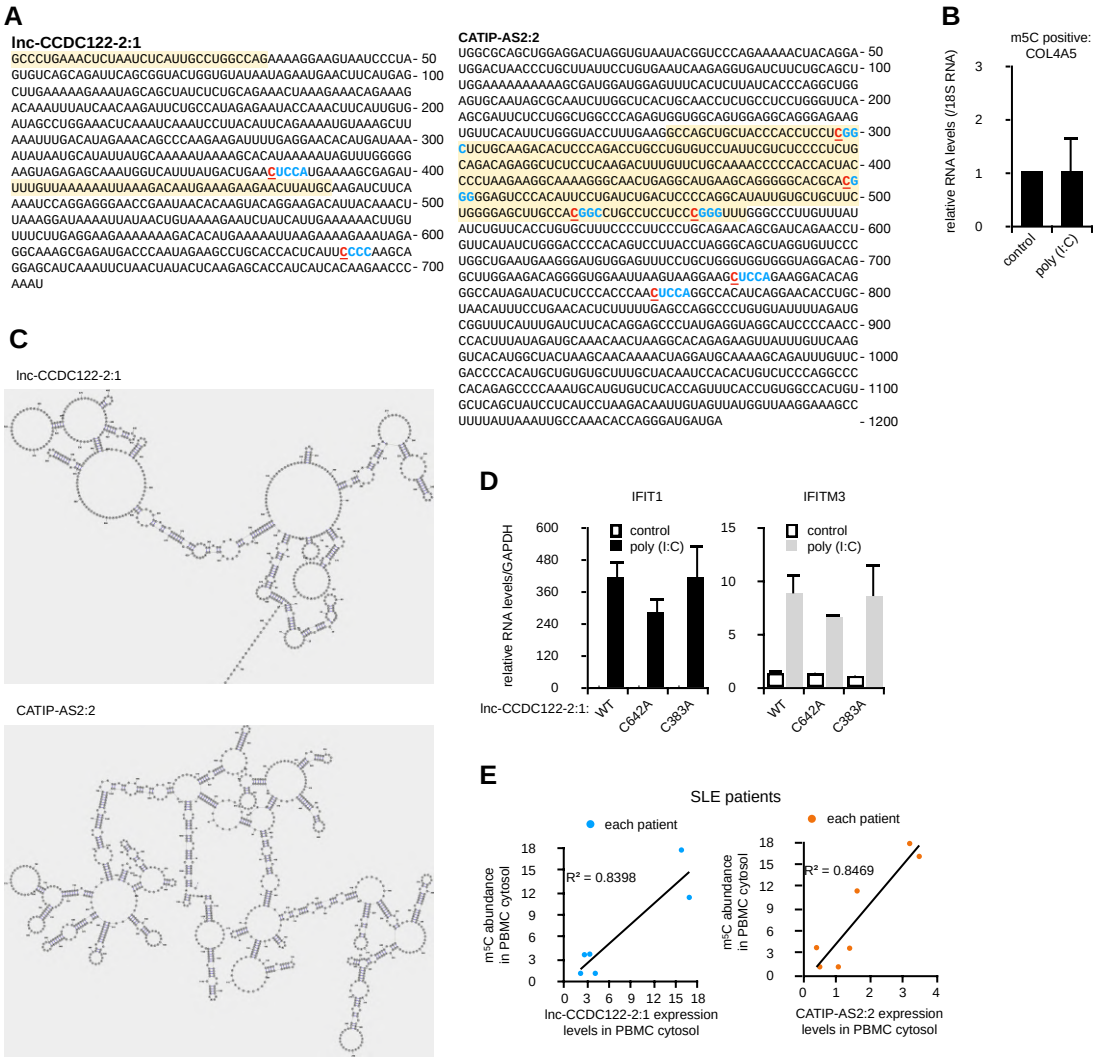


**Figure S8. Prediction of m5C-modification site on lnc-CCDC122-2:1 and CATIP-AS2:2.**

(**A)** Potential m$^5$C modification sites on lnc-CCDC122-2:1 and CATIP-AS2:2 are indicated in bold and underlined red, while the following sequences or motifs are indicated in bold blue. Both types of motifs have been identified and published [2,3]. Yellow-shaded region indicates previously reported RNA-m$^5$C modifications in lnc-CCDC122-2:1 and CATIP-AS2:2[4,5]. **(B)** Anti-m$^5$C-RNA immunoprecipitation (IP) in Huh7 cells with or without poly (I:C) transfection. Abundance of COL4A5 mRNA was measured in m$^5$C-immunoprecipitates by qRT-PCR. (**C**) Secondary structures of lnc-CCDC122-2:1 and CATIP-AS2:2 were predicted by REDfold. (**D**) Abundance of IFIT1 and IFITM3 mRNA was monitored in WT (n=3) Huh7 cells transfected with WT, C642A or C383A mutant of lnc-CCDC122-2:1. **(E)** Correlations between cytosolic m5C modified-RNA and cytosolic lnc-CCDC122-2:1 or CATIP-AS2:2 in SLE patients' PBMC (n=8).

1. Wang, L., Park, H.J., Dasari, S., Wang, S., Kocher, J.P., and Li, W. (2013). CPAT: Coding-Potential Assessment Tool using an alignment-free logistic regression model. Nucleic Acids Res *41*, e74. 10.1093/nar/gkt006.
2. Liu, J., Huang, T., Zhang, Y., Zhao, T., Zhao, X., Chen, W., and Zhang, R. (2020). Sequence- and structure-selective mRNA m5C methylation by NSUN6 in animals. National Science Review *8*. 10.1093/nsr/nwaa273.
3. Yang, X., Yang, Y., Sun, B.-F., Chen, Y.-S., Xu, J.-W., Lai, W.-Y., Li, A., Wang, X., Bhattarai, D.P., Xiao, W., et al. (2017). 5-methylcytosine promotes mRNA export — NSUN2 as the methyltransferase and ALYREF as an m5C reader. Cell Research *27*, 606-625. 10.1038/cr.2017.55.
4. Xue, C., Gu, X., Zheng, Q., Shi, Q., Yuan, X., Su, Y., Jia, J., Jiang, J., Lu, J., and Li, L. (2023). ALYREF mediates RNA m(5)C modification to promote hepatocellular carcinoma progression. Signal Transduct Target Ther *8*, 130. 10.1038/s41392-023-01395-7.
5. Chen, X., Li, A., Sun, B.F., Yang, Y., Han, Y.N., Yuan, X., Chen, R.X., Wei, W.S., Liu, Y., Gao, C.C., et al. (2019). 5-methylcytosine promotes pathogenesis of bladder cancer through stabilizing mRNAs. Nat Cell Biol *21*, 978-990. 10.1038/s41556-019-0361-y.